Measurement of the *b*-Quark Production Cross Section in 7 and 13 TeV *pp* Collisions

R. Aaij *et al.*[*]

(LHCb Collaboration)

Measurements of the cross section for producing *b* quarks in the reaction $pp \to b\bar{b}X$ are reported in 7 and 13 TeV collisions at the LHC as a function of the pseudorapidity η in the range $2 < \eta < 5$ covered by the acceptance of the LHCb experiment. The measurements are done using semileptonic decays of *b*-flavored hadrons decaying into a ground-state charmed hadron in association with a muon. The cross sections in the covered η range are $72.0 \pm 0.3 \pm 6.8$ and $154.3 \pm 1.5 \pm 14.3$ μb for 7 and 13 TeV. The ratio is $2.14 \pm 0.02 \pm 0.13$, where the quoted uncertainties are statistical and systematic, respectively. The agreement with theoretical expectation is good at 7 TeV, but differs somewhat at 13 TeV. The measured ratio of cross sections is larger at lower η than the model prediction.

Production of *b* quarks in high energy *pp* collisions at the LHC provides a sensitive test of models based on quantum chromodynamics [1]. Searches for physics beyond the standard model (SM) often rely on the ability to accurately predict the production rates of *b* quarks that can form backgrounds in combination with other high energy processes [2]. In addition, knowledge of the *b*-quark yield is essential for calculating the sensitivity of experiments testing the SM by measuring *CP*-violating and rare decay processes [3].

We present here measurements of production cross sections for the average of *b*-flavored and $\bar{b}$-flavored hadrons, denoted $pp \to H_b X$, where X indicates additional particles, in *pp* collisions recorded by LHCb at both 7 and 13 TeV center-of-mass energies, and their ratio. These measurements are made as a function of the H_b pseudorapidity η in the interval $2 < \eta < 5$, where $\eta = -\ln[\tan(\theta/2)]$, and θ is the angle of the weakly decaying *b* or $\bar{b}$ hadron with respect to the proton direction. We report results over the full range of *b*-hadron transverse momentum, p_T. The H_b cross section has been previously measured at LHCb in 7 TeV collisions using semileptonic decays to $D^0\mu^-X$ [4] and $b \to J/\psi X$ decays [5]. Previous determinations were made at the Tevatron collider in $\bar{p}p$ collisions near 2 TeV center-of-mass energy [6]. Other LHC experiments have also measured *b*-quark production characteristics at 7 [7], and 13 TeV [8]. The method presented in this Letter is more accurate because the normalization is based on well-measured semileptonic $\bar{B}^0$ and B^- branching fractions, and the equality of semileptonic widths for all *b* hadrons, in contrast to inclusive J/ψ production which relies on the assumption that the *b*-hadron

[*]Full author list given at end of the article.

particle species are produced in the same proportions as at LEP [9], or those that just use one specific *b* hadron, which needs the *b*-hadron fractions to extrapolate to the total.

The production cross section for a hadron H_b that contains either a *b* or $\bar{b}$ quark, but not both, is given by

$$\sigma(pp \to H_b X) = \frac{1}{2}[\sigma(B^0) + \sigma(\overline{B}^0)] + \frac{1}{2}[\sigma(B^+) + \sigma(B^-)]$$
$$+ \frac{1}{2}[\sigma(B_s^0) + \sigma(\overline{B}_s^0)]$$
$$+ \frac{1+\delta}{2}[\sigma(\Lambda_b^0) + \sigma(\overline{\Lambda}_b^0)], \tag{1}$$

where δ is a correction that accounts for Ξ_b and Ω_b^- baryons; we ignore B_c mesons since their production level is estimated to be only 0.1% of *b* hadrons [10].

Our estimate of δ is based on a paper by Voloshin [11], in which two useful relations are given:

$$\Gamma(\Xi_b^- \to \Xi^- X\mu^-\overline{\nu}) = \Gamma(\Lambda_b^0 \to \Lambda X\mu^-\overline{\nu}),$$
$$\text{and} \quad \frac{\sigma(\Xi_b^-)}{\sigma(\Lambda_b^0)} = 0.11 \pm 0.03 \pm 0.03, \tag{2}$$

where the latter is determined from Tevatron data, and the second uncertainty is assigned from the allowable SU(3) symmetry breaking. The *b*-hadron fractions determined there [9] agree with the ones measured by LHCb for other *b*-flavored hadrons [12]. Since the lifetimes of the Λ_b^0 and Ξ_b^- are equal within their uncertainties [9], assuming that the two branching fractions are equal gives us an estimate of 0.11 for the Ξ_b^-/Λ_b^0 semileptonic decay ratio. However, this must be doubled, using isospin invariance, to account for the Ξ_b^0. To this we must add the Ω_b^- contribution, taken as 15% of the Ξ_b, thus arriving at an estimate of δ of 0.25 ± 0.10, where the uncertainty is the one in Eq. (2)

TABLE I.   Measured semileptonic decay branching fractions for $\bar{B}^0$ and B^- mesons. The correlation of the errors in the underlying measurements in the average is taken into account. The CLEO numbers result from solving Eq. (4).

$\mathcal{B}_{SL}^0$ (%)	$\mathcal{B}_{SL}^-$ (%)	Source
10.49 ± 0.27	11.31 ± 0.27	CLEO [17]
9.64 ± 0.43	10.28 ± 0.47	BABAR [18]
10.46 ± 0.38	11.17 ± 0.38	Belle [19]
10.31 ± 0.19	11.09 ± 0.20	Average

added in quadrature to our estimate of the uncertainties from assuming isospin and lifetime equalities.

To measure these cross sections we determine the signal yields of b decays into a charm hadron plus a muon for a given integrated luminosity $\mathcal{L}$ and correct for various efficiencies described below. Explicitly,

$$
\sigma(pp \rightarrow H_b X)
$$
$$
= \frac{1}{2\mathcal{L}} \left[\left(\frac{n(D^0\mu)}{\epsilon_{D^0} \times \mathcal{B}_{D^0}} + \frac{n(D^+\mu)}{\epsilon_{D^+} \times \mathcal{B}_{D^+}} \right) \frac{1}{\mathcal{B}(B \rightarrow DX\mu\nu)} \right.
$$
$$
+ \left(\frac{n(D_s^+\mu)}{\epsilon_{D_s^+} \times \mathcal{B}_{D_s^+}} \right) \frac{1}{\mathcal{B}(B_s \rightarrow D_s X\mu\nu)}
$$
$$
\left. + \left(\frac{n(\Lambda_c^+\mu)}{\epsilon_{\Lambda_c^+} \times \mathcal{B}_{\Lambda_c^+}} \right) \frac{1+\delta}{\mathcal{B}(\Lambda_b^0 \rightarrow \Lambda_c^+ X\mu\nu)} \right], \quad (3)
$$

where $n(X_c\mu)$ means the number of detected charm hadron plus muon events and their charge conjugates, with corresponding efficiencies denoted by ϵ_{X_c}. The charm branching fractions, $\mathcal{B}_{X_c}$, used in this analysis, along with their sources, are listed in the Supplemental Material [13]. The PDG average is used for the D^0 and D_s^+ modes [9]. For the D^+ mode there is only one measurement by CLEO III, so that is used [14]. For the Λ_c^+ we average measurements by BES III [15] and Belle [16]. The expression $\mathcal{B}(B \rightarrow DX\mu\nu)$ denotes the average branching fraction for $\bar{B}^0$ and B^- semileptonic decays.

The $\bar{B}^0$ and B^- semileptonic branching fractions are obtained with a somewhat different procedure than that adopted by the PDG, whose actual estimate is difficult to derive from the posted information. We take three

measurements that are mostly model independent and average them. The first one was made by CLEO using inclusive leptons at the $\Upsilon(4S)$ resonance without distinguishing whether they are from $\bar{B}^0$ or B^- meson decays [17]. The $\Upsilon(4S)$, however, does not have an equal branching fraction into $\bar{B}^0 B^0$ and $B^- B^+$ mesons. In fact the fraction into neutral B pairs is $\alpha = 0.486 \pm 0.006$ [9], with the remainder going into charged B pairs. Therefore, to compute the $\bar{B}^0$ and B^- semileptonic branching fractions we need to use the following coupled equations

$$
\alpha\mathcal{B}_{SL}^0 + (1-\alpha)\mathcal{B}_{SL}^- = (10.91 \pm 0.09 \pm 0.24)\%,
$$
$$
\mathcal{B}_{SL}^0 / \mathcal{B}_{SL}^- = \tau^0/\tau^- = 0.927 \pm 0.004, \quad (4)
$$

where τ^i are the lifetimes [9]. The numbers extracted from the solution are listed in Table I, along with direct measurements from CLEO [17], BABAR [18], and Belle [19]. These latter two analyses measure the semileptonic decays of $\bar{B}^0$ and B^- mesons separately. They do not cover the full momentum range so a correction has to be applied; this was done by the PDG [9]. Since D^0 and D^+ mesons are produced in both $\bar{B}^0$ and B^- decays, we sum their yields and use the average semileptonic branching fraction for $\bar{B}^0$ and B^- decays, $\langle \bar{B}^0 + B^- \rangle$.

The semileptonic B branching fractions we use are listed in Table II. Since we are detecting only $b \rightarrow c\mu\nu$ modes, we have to correct later for the fact that there is a small 1% $b \rightarrow u\mu\nu$ component [9].

The semileptonic widths Γ_{SL} are equal for all H_b species used in this analysis except for a small correction for Λ_b^0 decays ($\mathcal{B}_{SL} = \Gamma_{SL}/\Gamma = \Gamma_{SL} \times \tau$). This has proven to be true in the case of charm hadron decays even though the lifetimes of D^0 and D^+ differ by a factor of 2.5. The decays of the Λ_b^0 are slightly different due to the absence of the chromomagnetic correction that affects B-meson decays but is absent in b baryons [20–22]. Thus Γ_{SL}, and also $\mathcal{B}_{SL}$, are increased for the Λ_b^0 by $(4 \pm 2)\%$ [12].

The input for the $\bar{B}_s^0$ lifetime listed in Table II uses only measurements in the flavor-specific decay $\bar{B}_s^0 \rightarrow D_s^+ \pi^-$ from CDF [23] and LHCb [24]. Other measurements can in principle be used, e.g., in $J/\psi\phi$ or $J/\psi f_0(980)$ final states, but they then involve also determining $\Delta\Gamma_s$. Older measurements involving semileptonic decays are

TABLE II.   Measured semileptonic decay branching fractions for B mesons and derived branching fractions for $\bar{B}_s^0$ and Λ_b^0 based on the equality of semileptonic widths and the lifetime ratios.

Particle	τ (ps) measured	$\mathcal{B}_{SL}$ (%) measured	Γ_{SL} (ps^{-1}) measured	$\mathcal{B}_{SL}$ (%) to be used
$\bar{B}^0$	1.519 ± 0.005	10.31 ± 0.19	0.0678 ± 0.0013	10.31 ± 0.19
B^-	1.638 ± 0.004	11.09 ± 0.20	0.0680 ± 0.0013	11.09 ± 0.20
$\langle \bar{B}^0 + B^- \rangle$		10.70 ± 0.19		10.70 ± 0.19
$\bar{B}_s^0$	1.533 ± 0.018			10.40 ± 0.30
Λ_b^0	1.467 ± 0.010			10.35 ± 0.28

suspected of having larger uncontrolled systematic uncertainties [25]. Finally, the Λ_b^0 lifetime is taken from the HFAG average [26].

Corrections due to cross feeds among the modes, for example, from $\overline{B}_s^0 \to DK\mu^- X$ events or $\Lambda_b^0 \to DN\mu^- X$ decays are well below our sensitivity, and thus we do not include them.

The data used here correspond to integrated luminosities of 284.10 ± 4.86 pb^{-1} collected at 7 TeV and 4.60 ± 0.18 pb^{-1} at 13 TeV [27], where special triggers were implemented to minimize uncertainties. The LHCb detector [28,29] is a single-arm forward spectrometer covering the pseudorapidity range $2 < \eta < 5$. Components include a high-precision tracking system consisting of a silicon-strip vertex detector surrounding the pp interaction region, a large-area silicon-strip detector located upstream of a dipole magnet with a bending power of about 4 Tm, and three stations of silicon-strip detectors and straw drift tubes placed downstream of the magnet. Different types of charged hadrons are distinguished using information from two ring-imaging Cherenkov detectors (RICH). Muons are identified by a system composed of alternating layers of iron and multiwire proportional chambers.

Events of potential interest are triggered by the identification of a muon in real time with a minimum p_T of 1.48 GeV in the 7 TeV data [30], and 0.9 GeV in the 13 TeV data (further restricted in the higher level trigger to $p_T > 1.3$ GeV) [31]. In addition, to test for inconsistency with production at the primary vertex (PV), the $\chi_{\rm IP}^2$ for the muon is computed as the difference between the vertex fit χ^2 of the PV reconstructed with and without the considered track. We require that $\chi_{\rm IP}^2$ be larger than 200 at 7 TeV (16 at 13 TeV), and in the 7 TeV data only, the impact parameter of the muon must be greater than 0.5 mm. There is a prescale by a factor of 2 for both energies and an additional prescale of a factor of 2 for the $D^0\mu^-$ channel in the 7 TeV data.

These events are subjected to further requirements in order to select those with a charmed hadron decay which forms a vertex with the identified muon that is detached from the PV. The charmed hadron must not be consistent with originating from the PV. We use the decays $D^0 \to K^-\pi^+$, $D^+ \to K^-\pi^+\pi^+$, $D_s^+ \to K^+K^-\pi^+$, and $\Lambda_c^+ \to pK^-\pi^+$. (The related branching fractions are given in the Supplemental Material [13]). The RICH system is used to determine a likelihood for each particle hypothesis. We use selections on the differences of log-likelihoods ($\mathcal{L}$) to separate protons from kaons and pions, $\mathcal{L}(p) - \mathcal{L}(K) > 0$ and $\mathcal{L}(p) - \mathcal{L}(\pi) > 10$, kaons from pions $\mathcal{L}(K) - \mathcal{L}(\pi) > 4$, and pions from kaons $\mathcal{L}(K) - \mathcal{L}(\pi) < 4$ for 7 and < 10 for 13 TeV. In addition, in order to suppress background, the average p_T of the charm hadron daughters must be larger than 700 MeV for three-body and 600 MeV for two-body decays, and the invariant mass of the charm hadron plus muon must range from approximately 3 to

5 GeV. Furthermore, the charm plus μ vertex must be within a radius less than 4.8 mm from the beam line to remove contributions of secondary interactions in the detector material due to long-lived particles, and the charm hadron must decay downstream of this vertex.

Since detection efficiencies vary over the available phase space, we divide the data into two-dimensional intervals in p_T of the charm plus μ system, and η, where the latter is determined from the relative positions of the charm plus μ vertex and the PV. We fit the data for each charm plus μ combination in each interval simultaneously in invariant mass of the charm hadron and $\ln(IP/\text{mm})$ variables, where IP is the measured impact parameter of the charmed hadron with respect to the PV in units of mm.

As an example of the fitting technique consider $D_s^+\mu^-$ candidates integrated over p_T and η for the 7 TeV data. Figure 1(a) shows the $K^+K^-\pi^+$ invariant mass spectrum, while (b) shows the $\ln(IP/\text{mm})$ distribution. The invariant mass signal is fit for the D_s^+ yield with a double-Gaussian function where the means of the two Gaussians are constrained to be the same. The common mean and the widths are determined in the fit. (A second double-Gaussian shape is used to fit the higher mass decay of $D^{*+} \to \pi^+D^0$, $D^0 \to K^+K^-$, an additional consideration only in this mode.) The $\ln(IP/\text{mm})$ shape of the signal component, determined by simulation, is a bifurcated Gaussian where the peak position and width parameters are determined by the fit. The combinatorial background is modeled with a linear shape. (The other modes at both energies are shown in the Supplemental Material [13].) The signal yields for charm hadron plus muon candidates integrated over η are also given in the Supplemental Material [13].

The major components of the total efficiency are the off-line and trigger efficiencies. The latter is measured with respect to the off-line, which has several components from tracking, particle identification, event selection, and overall event size cuts. These have been evaluated in a data-driven manner whenever possible. Only the event selection efficiencies have been simulated. Samples of simulated events, produced with the software described in Refs. [32–34], are used to characterize signal and background contributions. The particle identification efficiencies are determined from calibration samples of $D^{*+} \to \pi^+D^0$, $D^0 \to K^-\pi^+$ decays for kaons and pions, and $\Lambda \to p\pi^-$ for protons. The trigger efficiencies including the muon identification efficiency are determined using samples of $b \to J/\psi X$, $J/\psi \to \mu^+\mu^-$ decays, where one muon is identified and the other used to measure the efficiencies. For the overall sample they are typically 20% for the 7 TeV data and 70% for the 13 TeV data, only weakly dependent on η. The difference is caused primarily by the impact parameter cut on the muon of 0.5 mm in the 7 TeV data. The efficiency for the overall event size requirement is determined using $B^- \to J/\psi K^-$ decays where much looser criteria were applied. These efficiencies are all above 95% and are determined with
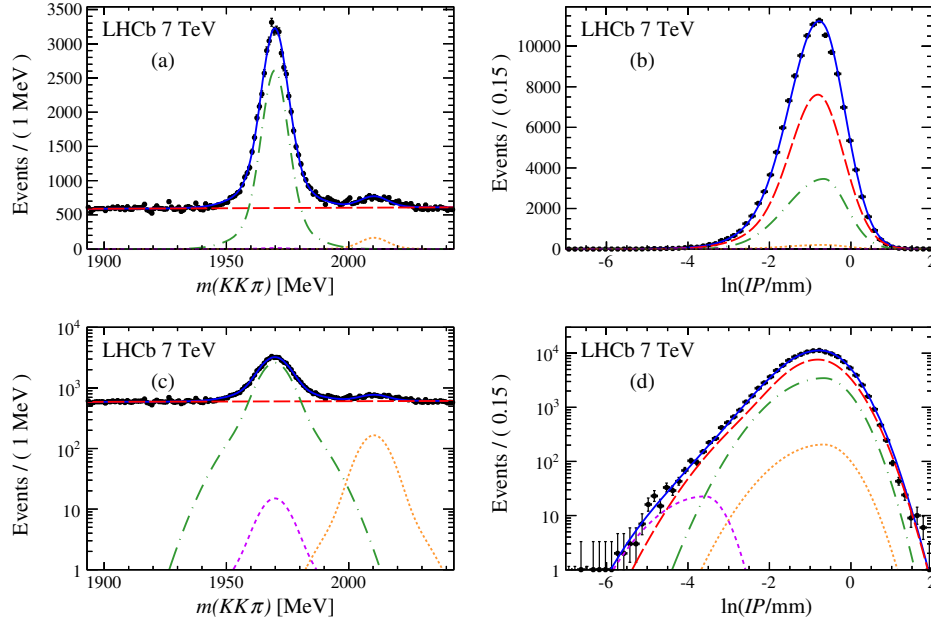
FIG. 1.   Fits to the $K^+K^-\pi^+$ invariant mass (a) and $\ln(IP/\mathrm{mm})$ (b) distributions for data taken at 7 TeV data integrated over $2 < \eta < 5$. The data are shown as solid circles (black), and the overall fits as solid lines (blue). The dot-dashed (green) curve shows the D_s^+ signal from b decay, while the dashed (purple) curve D_s^+ from prompt production. The dotted curve (orange) shows the D^{*+} component. The dashed line (red) shows the combinatorial background. The same fits using a logarithmic scale are shown in (c) and (d).

negligible uncertainties. The total efficiencies given as a function of η and p_T for both energies are shown in the Supplemental Material [13].

There is dwindling efficiency toward small p_T values of the charmed hadron plus muon. Data in the regions with negligible efficiency are excluded, and a correction is made using simulation to calculate the fraction of events that fall within inefficient regions. These numbers are calculated for each bin of η for 7 and 13 TeV data separately, and the averages are 38% at 7 TeV and 46% at 13 TeV. The p_T distributions from simulation in each η bin have been checked and found to agree within error with those observed in the data in bins with sufficient statistics.

The signal yields are obtained from fits that subtract the uncorrelated backgrounds. There are, however, two background sources that must be dealt with separately. One results from real charm hadron decays that form a vertex with a charged track that is misidentified as a muon and the other is from b decays into two charmed hadrons where one decays either leptonically or semileptonically into a muon. In most cases the requirement that the muon forms a vertex with the charmed hadron eliminates this background, but some remains. The background from fake muons combined with a real charmed hadron, and a real muon combined with a charm hadron from another b decay as estimated from wrong-sign muon and hadron combinations is 0.7% at 7 TeV and 2.0% at 13 TeV. The fake rates caused by b decays to two charmed hadrons where one decays semileptonically have been evaluated from simulation and are about 2% when averaged over all charmed species.

The inclusive b-hadron cross sections as functions of η are given in Fig. 2, along with a theoretical prediction called FONLL [35]. These results are consistent with and supersede our previous results at 7 TeV [4]. The ratio of cross sections is predicted with less uncertainty, and indeed most of the experimental uncertainties (discussed below) also cancel, with the largest exception being the luminosity error. In Fig. 2(c), we compare the η-dependent cross-section ratio for 13 TeV divided by 7 TeV with the FONLL prediction. We see higher ratios at lower values of η than given by the prediction, which indicates that the cross section at η values near 2 is growing faster than at larger values.

The results as a function of η are listed in Table III. The total cross sections at 7 and 13 TeV integrated over $2 < \eta < 5$ are $72.0 \pm 0.3 \pm 6.8$ and $154.3 \pm 1.5 \pm 14.3$ μb for 7 and 13 TeV. The ratio is $2.14 \pm 0.02 \pm 0.13$. This agrees with the theoretical prediction at 7 TeV of 62^{+28}_{-22} μb, and is a bit larger than the 13 TeV prediction of 111^{+51}_{-44} μb. While the measured ratio is consistent with the prediction of $1.79^{+0.21}_{-0.15}$, it disagrees with the combination of shape and normalization.

Systematic uncertainties are considerably larger than the statistical errors. The ones that are independent of η are listed in Table IV. The luminosity and muon trigger efficiency uncertainties in the ratio are each obtained by assuming a -50% correlated error [36]. The uncertainty in the tracking efficiency is given by taking 0.5% per muon track and 1.5% per hadron track [37]. The various final states used to simulate the efficiencies can contribute to an overall efficiency change. This is estimated by taking the
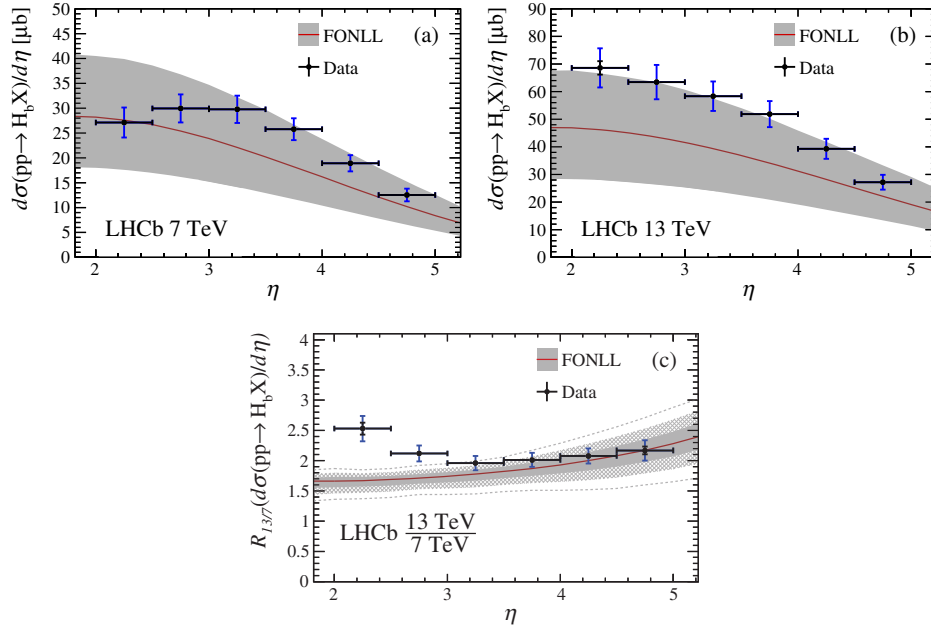
FIG. 2.   The differential cross section as a function of η for $\sigma(pp \to H_b X)$, where H_b is a hadron that contains either a b or a $\bar{b}$ quark, but not both, at center-of-mass energies of 7 TeV (a) and 13 TeV (b). The ratio is shown in (c). The smaller error bars (black) show the statistical uncertainties only, and the larger ones (blue) have the systematic uncertainties added in quadrature. The solid line (red) gives the theoretical prediction, while the solid shaded band gives the estimated uncertainty on the predictions at $\pm 1\sigma$, the cross-hatched at $\pm 2\sigma$, and the dashes at $\pm 3\sigma$.

difference between the efficiencies of the higher multiplicity $D^*\mu^-\nu$ states and $D^{**}\mu^-\nu$ states, where D^{**} refers to excited states that decay into a charmed particle and pions, and taking into account the uncertainties on the measured branching fractions. These are then added in quadrature and referred to as the b decay cocktail in Table IV.

The fraction of higher mass b-baryon states with respect to the Λ_b^0 is given by $\delta = 0.25 \pm 0.10$, which represents a 40% relative uncertainty that affects only the baryon contribution to Eq. (3).

There are also η-dependent systematic uncertainties in the cross section that arise from the trigger efficiency, the event selection, the hadron identification, and the corrections for the low p_T region with low efficiencies. When added in quadrature with the η-independent uncertainties, the total errors range from (8.5–11.0)% at 7 TeV to

(8.7–9.7)% at 13 TeV. There is some cancellation in the ratio giving a range of (5.6–7.3)%.

In conclusion, new results for the $b\bar{b}$ production cross section at 7 TeV are in good agreement with the original η-dependent cross-section measurement previously reported [4], and are in agreement with the theoretical prediction (FONLL) [35]. The 13 TeV results are somewhat higher in magnitude than the theory, and generally agree with the shape and magnitude measured using inclusive $b \to J/\psi X$ decays [36]. The cross-section ratio of 13 to 7 TeV as a function of η differs from the FONLL model by 5 standard deviations, including the systematic uncertainties. This discrepancy is mainly the difference in the low η bins. To get an idea of the cross section in the full η range we use

TABLE IV.   Systematic uncertainties independent of η on the $pp \to H_b X$ cross sections at 7 and 13 TeV and their ratio.

Source	7 TeV	13 TeV	Ratio 13/7
Luminosity	1.7%	3.9%	3.8%
Tracking efficiency	3.8%	4.3%	2.5%
b semileptonic $\mathcal{B}$	2.1%	2.1%	0
Charm hadron $\mathcal{B}$	2.6%	2.6%	0
b decay cocktail	1.0%	1.0%	0
Ignoring b cross feeds	1.0%	1.0%	0
Background	0.2%	0.3%	0
$b \to u$ decays	0.3%	0.3%	0
δ	2.0%	2.0%	0.2%
Total	5.9%	7.1%	4.6%

TABLE III. $pp \to H_b X$ differential cross sections as a function of η for 7 and 13 TeV collisions and their ratio. The first uncertainty is statistical and the second systematic. To get the cross section in each interval divide by a factor of 2.

η	7 TeV (μb)	13 TeV (μb)	Ratio 13/7
2.0–2.5	$27.2 \pm 0.5 \pm 3.0$	$68.6 \pm 2.4 \pm 6.7$	$2.53 \pm 0.10 \pm 0.18$
2.5–3.0	$29.9 \pm 0.2 \pm 2.8$	$63.4 \pm 0.9 \pm 6.2$	$2.12 \pm 0.03 \pm 0.13$
3.0–3.5	$29.8 \pm 0.2 \pm 2.7$	$58.3 \pm 1.0 \pm 5.3$	$1.96 \pm 0.04 \pm 0.11$
3.5–4.0	$25.8 \pm 0.2 \pm 2.2$	$51.9 \pm 0.7 \pm 4.7$	$2.01 \pm 0.03 \pm 0.11$
4.0–4.5	$18.9 \pm 0.1 \pm 1.6$	$39.3 \pm 0.6 \pm 3.6$	$2.08 \pm 0.04 \pm 0.12$
4.5–5.0	$12.5 \pm 0.1 \pm 1.3$	$27.2 \pm 0.7 \pm 2.6$	$2.17 \pm 0.06 \pm 0.16$

multiplicative factors derived from Pythia 8 simulations of 4.1 at 7 TeV and 3.9 at 13 TeV [33,34] and extrapolate the total $b\bar{b}$ cross sections as ≈ 295 μb at 7 TeV and ≈ 600 μb at 13 TeV.

[1] M. Cacciari, S. Frixione, N. Houdeau, M. L. Mangano, P. Nason, and G. Ridolfi, Theoretical predictions for charm and bottom production at the LHC, J. High Energy Phys. 10 (2012) 137; B. A. Kniehl, G. Kramer, I. Schienbein, and H. Spiesberger, Inclusive B-meson production at the LHC in the GM-VFN scheme, Phys. Rev. D **84**, 094026 (2011).

[2] E. Halkiadakis, G. Redlinger, and D. Shih, Status and implications of beyond-the-standard-model searches at the LHC, Annu. Rev. Nucl. Part. Sci. **64**, 319 (2014).

[3] R. Aaij et al. (LHCb Collaboration), Implications of LHCb measurements and future prospects, Eur. Phys. J. C **73**, 2373 (2013).

[4] R. Aaij et al. (LHCb Collaboration), Measurement of $\sigma(pp \to b\bar{b}X)$ at $\sqrt{s} = 7$ TeV in the forward region, Phys. Lett. B **694**, 209 (2010).

[5] R. Aaij et al. (LHCb Collaboration), Measurement of J/ψ production in pp collisions at $\sqrt{s} = 7$ TeV, Eur. Phys. J. C **71**, 1645 (2011).

[6] B. Abbott et al. (D0 Collaboration), The $b\bar{b}$ production cross section and angular correlations in $p\bar{p}$ collisions at $\sqrt{s} = 1.8$ TeV, Phys. Lett. B **487**, 264 (2000); T. Aaltonen et al. (CDF Collaboration), Measurement of the b-hadron production cross section using decays to $\mu - D^0 X$ final states in $p\bar{p}$ collisions at $\sqrt{s} = 1.96$ TeV, Phys. Rev. D **79**, 092003 (2009); T. Aaltonen et al. (CDF Collaboration), Measurement of correlated $b\bar{b}$ production in $p^- \bar{p}$ collisions at $\sqrt{s} = 1960$ GeV, Phys. Rev. D **77**, 072004 (2008).

[7] S. Chatrchyan et al. (CMS Collaboration), Measurement of the strange B meson production cross section with $J/\psi\phi$ decays in pp collisions at $\sqrt{s} = 7$ TeV, Phys. Rev. D **84**, 052008 (2011); R. Aaij et al. (LHCb Collaboration), Measurement of the $B^{\pm}$ production cross-section in pp collisions at $\sqrt{s} = 7$ TeV, J. High Energy Phys. 04 (2012) 093; S. Chatrchyan et al. (CMS Collaboration), Measurement of the cross section for production of $b\bar{b}X$, decaying to muons in pp collisions at $\sqrt{s} = 7$ TeV, J. High Energy Phys. 06 (2012) 110; S. Chatrchyan et al. (CMS Collaboration), Measurement of the Λ_b^0 cross section and the $\overline{\Lambda_b^0}$ to Λ_b^0 ratio with $J/\psi\Lambda$ decays in pp collisions at $\sqrt{s} = 7$ TeV, Phys. Lett. B **714**, 136 (2012); B. Abelev et al. (ALICE Collaboration), Measurement of prompt J/ψ and beauty hadron production cross sections at mid-rapidity in pp collisions at $\sqrt{s} = 7$ TeV, J. High Energy Phys. 11 (2012) 065; G. Aad et al. (ATLAS Collaboration), Measurement of the b-hadron production cross section using decays to $D^{*}\mu^- X$ final states in pp collisions at $\sqrt{s} = 7$ TeV with the ATLAS detector, Nucl. Phys. **B864**, 341 (2012); G. Aad et al. (ATLAS Collaboration), Measurement of the differential cross-section of B^+ meson production in pp collisions at $\sqrt{s} = 7$ TeV at ATLAS, J. High Energy Phys. 10 (2013) 042; R. Aaij et al. (LHCb Collaboration), Measurement of B meson production cross-sections in proton-proton collisions at $\sqrt{s} = 7$ TeV, J. High Energy Phys. 08 (2013) 117.

[8] V. Khachatryan et al. (CMS Collaboration), Measurement of the total and differential inclusive B^+ hadron cross sections in pp collisions at $\sqrt{s} = 13$ TeV, arXiv: 1609.00873 [Phys. Lett. B (to be published)].

[9] K. A. Olive et al. (Particle Data Group), Review of particle physics, Chin. Phys. C **38**, 090001 (2014), and 2015 online update.

[10] R. Aaij et al. (LHCb Collaboration), Precision Measurement of CP Violation in $B_s^0 \to J/\psi K^+ K^-$ Decays, Phys. Rev. Lett. **114**, 041801 (2015).

[11] M. B. Voloshin, Remarks on measurement of the decay $\Xi_b^- \to \Lambda_b^0 \pi^-$, arXiv:1510.05568.

[12] R. Aaij et al. (LHCb Collaboration), Measurement of b-hadron production fractions in 7 TeV pp collisions, Phys. Rev. D **85**, 032008 (2012).

[13] See Supplemental Material at http://link.aps.org/supplemental/10.1103/PhysRevLett.118.052002 for the decay modes and charm hadronic branching fractions used in this analysis; The signal yields in the different b decay modes, fits to the different invariant mass spectra and ln (IP/mm) distributions for charm hadron plus muon events, and efficiencies for different η and p_T intervals.

[14] G. Bonvicini et al. (CLEO Collaboration), Updated measurements of absolute D^+ and D^0 hadronic branching fractions and $\sigma(e^+e^- \to D\overline{D})$ at $E_{cm} = 3774$ MeV, Phys. Rev. D **89**, 072002 (2014); Erratum, Phys. Rev. D **91**, 019903 (2015).

[15] M. Ablikim *et al.* (BESIII Collaboration), Measurements of Absolute Hadronic Branching Fractions of Λ_c^+ Baryon, Phys. Rev. Lett. **116**, 052001 (2016).

[16] A. Zupanc *et al.* (Belle Collaboration), Measurement of the Branching Fraction $B(\Lambda_c^+ \to pK^-\pi^+)$, Phys. Rev. Lett. **113**, 042002 (2014).

[17] A. H. Mahmood *et al.* (CLEO Collaboration), Measurement of the B-meson inclusive semileptonic branching fraction and electron energy moments, Phys. Rev. D **70**, 032003 (2004).

[18] B. Aubert *et al.* (*BABAR* Collaboration), Measurement of the ratio $\mathcal{B}(B^+ \to Xe\nu)/\mathcal{B}(B^0 \to Xe\nu)$, Phys. Rev. D **74**, 091105 (2006).

[19] P. Urquijo *et al.* (Belle Collaboration), Moments of the electron energy spectrum and partial branching fraction of $B \to X(c)e\nu$ decays at Belle, Phys. Rev. D **75**, 032001 (2007).

[20] A. V. Manohar and M. B. Wise, Inclusive semileptonic B and polarized Λ_b^0 decays from QCD, Phys. Rev. D **49**, 1310 (1994).

[21] I. I. Bigi, M. A. Shifman, N. G. Uraltsev, and A. I. Vainshtein, QCD Predictions for Lepton Spectra in Inclusive Heavy Flavor Decays, Phys. Rev. Lett. **71**, 496 (1993).

[22] I. I. Bigi, T. Mannel, and N. Uraltsev, Semileptonic width ratios among beauty hadrons, J. High Energy Phys. 09 (2011) 012.

[23] T. Aaltonen *et al.* (CDF Collaboration), Measurement of the B_s Lifetime in Fully and Partially Reconstructed $B_s \to D_s^-(\phi\pi^-)X$ Decays in $\overline{p} - p$ Collisions at $\sqrt{s} = 1.96$ TeV, Phys. Rev. Lett. **107**, 272001 (2011).

[24] R. Aaij *et al.* (LHCb Collaboration), Measurement of the $\overline{B}_s^0$ Meson Lifetime in $D_s^+\pi^-$ Decays, Phys. Rev. Lett. **113**, 172001 (2014).

[25] S. Stone, Lifetimes of some b-flavored hadrons, in 12th Conference on Flavor Physics and *CP* Violation (FPCP 2014) Marseille, France, May 26-30, 2014, 2014, arXiv:1406.6497.

[26] Y. Amhis *et al.* (Heavy Flavor Averaging Group), Averages of b-hadron, c-hadron, and τ-lepton properties as of summer 2014 and online update at http://www.slac.stanford.edu/xorg/hfag, arXiv:1412.7515, updated results and plots available at http://www.slac.stanford.edu/xorg/hfag/.

[27] R. Aaij *et al.* (LHCb Collaboration), Precision luminosity measurements at LHCb, J. Instrum. **9**, P12005 (2014).

[28] A. A. Alves Jr. *et al.* (LHCb Collaboration), The LHCb detector at the LHC, J. Instrum. **3**, S08005 (2008).

[29] R. Aaij *et al.* (LHCb Collaboration), LHCb detector performance, Int. J. Mod. Phys. A **30**, 1530022 (2015).

[30] R. Aaij *et al.*, The LHCb trigger and its performance in 2011, J. Instrum. **8**, P04022 (2013).

[31] R. Aaij *et al.*, Tesla: An application for real-time data analysis in high energy physics, Comput. Phys. Commun. **208**, 35 (2016).

[32] T. Sjostrand, S. Mrenna, and P. Z. Skands, PYTHIA 6.4 physics and manual, J. High Energy Phys. 05 (2006) 026.

[33] T. Sjöstrand, S. Mrenna, and P. Skands, A brief introduction to PYTHIA 8.1, Comput. Phys. Commun. **178**, 852 (2008).

[34] I. Belyaev *et al.*, Handling of the generation of primary events in Gauss, the LHCb simulation framework, J. Phys. Conf. Ser. **331**, 032047 (2011); D. J. Lange, The EvtGen particle decay simulation package, Nucl. Instrum. Methods Phys. Res., Sect. A **462**, 152 (2001); P. Golonka and Z. Was, PHOTOS Monte Carlo: A precision tool for QED corrections in Z and W decays, Eur. Phys. J. C **45**, 97 (2006); J. Allison *et al.*, Geant4 developments and applications, IEEE Trans. Nucl. Sci. **53**, 270 (2006); S. Agostinelli *et al.* (GEANT4 Collaboration), GEANT4: A simulation toolkit, Nucl. Instrum. Methods Phys. Res., Sect. A **506**, 250 (2003); M. Clemencic *et al.* (LHCb Collaboration), The LHCb simulation application, Gauss: Design, evolution and experience, J. Phys. Conf. Ser. **331**, 032023 (2011).

[35] M. Cacciari, M. L. Mangano, and P. Nason, Gluon PDF constraints from the ratio of forward heavy-quark production at the LHC at $\sqrt{s} = 7$ and 13 TeV, Eur. Phys. J. C **75**, 610 (2015).

[36] R. Aaij *et al.* (LHCb Collaboration), Measurement of forward J/ψ production cross-sections in pp collisions at $\sqrt{s} = 13$ TeV, J. High Energy Phys. 10 (2015) 172.

[37] R. Aaij *et al.* (LHCb Collaboration), Measurement of the track reconstruction efficiency at LHCb, J. Instrum. **10**, P02007 (2015).

R. Aaij,[40] B. Adeva,[39] M. Adinolfi,[48] Z. Ajaltouni,[5] S. Akar,[6] J. Albrecht,[10] F. Alessio,[40] M. Alexander,[53] S. Ali,[43] G. Alkhazov,[31] P. Alvarez Cartelle,[55] A. A. Alves Jr.,[59] S. Amato,[2] S. Amerio,[23] Y. Amhis,[7] L. An,[41] L. Anderlini,[18] G. Andreassi,[41] M. Andreotti,[17,g] J. E. Andrews,[60] R. B. Appleby,[56] F. Archilli,[43] P. d'Argent,[12] J. Arnau Romeu,[6] A. Artamonov,[37] M. Artuso,[61] E. Aslanides,[6] G. Auriemma,[26] M. Baalouch,[5] I. Babuschkin,[56] S. Bachmann,[12] J. J. Back,[50] A. Badalov,[38] C. Baesso,[62] S. Baker,[55] W. Baldini,[17] R. J. Barlow,[56] C. Barschel,[40] S. Barsuk,[7] W. Barter,[40] M. Baszczyk,[27] V. Batozskaya,[29] B. Batsukh,[61] V. Battista,[41] A. Bay,[41] L. Beaucourt,[4] J. Beddow,[53] F. Bedeschi,[24] I. Bediaga,[1] L. J. Bel,[43] V. Bellee,[41] N. Belloli,[21,i] K. Belous,[37] I. Belyaev,[32] E. Ben-Haim,[8] G. Bencivenni,[19] S. Benson,[43] J. Benton,[48] A. Berezhnoy,[33] R. Bernet,[42] A. Bertolin,[23] F. Betti,[15] M.-O. Bettler,[40] M. van Beuzekom,[43] Ia. Bezshyiko,[42] S. Bifani,[47] P. Billoir,[8] T. Bird,[56] A. Birnkraut,[10] A. Bitadze,[56] A. Bizzeti,[18,u] T. Blake,[50] F. Blanc,[41] J. Blouw,[11,†] S. Blusk,[61] V. Bocci,[26] T. Boettcher,[58] A. Bondar,[36,w] N. Bondar,[31,40] W. Bonivento,[16] A. Borgheresi,[21,i] S. Borghi,[56] M. Borisyak,[35] M. Borsato,[39] F. Bossu,[7] M. Boubdir,[9] T. J. V. Bowcock,[54] E. Bowen,[42] C. Bozzi,[17,40] S. Braun,[12] M. Britsch,[12] T. Britton,[61] J. Brodzicka,[56] E. Buchanan,[48] C. Burr,[56] A. Bursche,[2] J. Buytaert,[40] S. Cadeddu,[16] R. Calabrese,[17,g] M. Calvi,[21,i] M. Calvo Gomez,[38,m]

A. Camboni,[38] P. Campana,[19] D. Campora Perez,[40] D. H. Campora Perez,[40] L. Capriotti,[56] A. Carbone,[15,e] G. Carboni,[25,j] R. Cardinale,[20,h] A. Cardini,[16] P. Carniti,[21,i] L. Carson,[52] K. Carvalho Akiba,[2] G. Casse,[54] L. Cassina,[21,i] L. Castillo Garcia,[41] M. Cattaneo,[40] Ch. Cauet,[10] G. Cavallero,[20] R. Cenci,[24,t] M. Charles,[8] Ph. Charpentier,[40] G. Chatzikonstantinidis,[47] M. Chefdeville,[4] S. Chen,[56] S.-F. Cheung,[57] V. Chobanova,[39] M. Chrzaszcz,[42,27] X. Cid Vidal,[39] G. Ciezarek,[43] P. E. L. Clarke,[52] M. Clemencic,[40] H. V. Cliff,[49] J. Closier,[40] V. Coco,[59] J. Cogan,[6] E. Cogneras,[5] V. Cogoni,[16,40,f] L. Cojocariu,[30] G. Collazuol,[23,o] P. Collins,[40] A. Comerma-Montells,[12] A. Contu,[40] A. Cook,[48] G. Coombs,[40] S. Coquereau,[38] G. Corti,[40] M. Corvo,[17,g] C. M. Costa Sobral,[50] B. Couturier,[40] G. A. Cowan,[52] D. C. Craik,[52] A. Crocombe,[50] M. Cruz Torres,[62] S. Cunliffe,[55] R. Currie,[55] C. D'Ambrosio,[40] F. Da Cunha Marinho,[2] E. Dall'Occo,[43] J. Dalseno,[48] P. N. Y. David,[43] A. Davis,[59] O. De Aguiar Francisco,[2] K. De Bruyn,[6] S. De Capua,[56] M. De Cian,[12] J. M. De Miranda,[1] L. De Paula,[2] M. De Serio,[14,d] P. De Simone,[19] C.-T. Dean,[53] D. Decamp,[4] M. Deckenhoff,[10] L. Del Buono,[8] M. Demmer,[10] D. Derkach,[35] O. Deschamps,[5] F. Dettori,[40] B. Dey,[22] A. Di Canto,[40] H. Dijkstra,[40] F. Dordei,[40] M. Dorigo,[41] A. Dosil Suárez,[39] A. Dovbnya,[45] K. Dreimanis,[54] L. Dufour,[43] G. Dujany,[56] K. Dungs,[40] P. Durante,[40] R. Dzhelyadin,[37] A. Dziurda,[40] A. Dzyuba,[31] N. Déléage,[4] S. Easo,[51] M. Ebert,[52] U. Egede,[55] V. Egorychev,[32] S. Eidelman,[36,w] S. Eisenhardt,[52] U. Eitschberger,[10] R. Ekelhof,[10] L. Eklund,[53] Ch. Elsasser,[42] S. Ely,[61] S. Esen,[12] H. M. Evans,[49] T. Evans,[57] A. Falabella,[15] N. Farley,[47] S. Farry,[54] R. Fay,[54] D. Fazzini,[21,i] D. Ferguson,[52] V. Fernandez Albor,[39] A. Fernandez Prieto,[39] F. Ferrari,[15,40] F. Ferreira Rodrigues,[1] M. Ferro-Luzzi,[40] S. Filippov,[34] R. A. Fini,[14] M. Fiore,[17,g] M. Fiorini,[17,g] M. Firlej,[28] C. Fitzpatrick,[41] T. Fiutowski,[28] F. Fleuret,[7,b] K. Fohl,[40] M. Fontana,[16,40] F. Fontanelli,[20,h] D. C. Forshaw,[61] R. Forty,[40] V. Franco Lima,[54] M. Frank,[40] C. Frei,[40] J. Fu,[22,q] E. Furfaro,[25,j] C. Färber,[40] A. Gallas Torreira,[39] D. Galli,[15,e] S. Gallorini,[23] S. Gambetta,[52] M. Gandelman,[2] P. Gandini,[57] Y. Gao,[3] L. M. Garcia Martin,[68] J. García Pardiñas,[39] J. Garra Tico,[49] L. Garrido,[38] P. J. Garsed,[49] D. Gascon,[38] C. Gaspar,[40] L. Gavardi,[10] G. Gazzoni,[5] D. Gerick,[12] E. Gersabeck,[12] M. Gersabeck,[56] T. Gershon,[50] Ph. Ghez,[4] S. Gianì,[41] V. Gibson,[49] O. G. Girard,[41] L. Giubega,[30] K. Gizdov,[52] V. V. Gligorov,[8] D. Golubkov,[32] A. Golutvin,[55,40] A. Gomes,[1,a] I. V. Gorelov,[33] C. Gotti,[21,i] M. Grabalosa Gándara,[5] R. Graciani Diaz,[38] L. A. Granado Cardoso,[40] E. Graugés,[38] E. Graverini,[42] G. Graziani,[18] A. Grecu,[30] P. Griffith,[47] L. Grillo,[21,40,i] B. R. Gruberg Cazon,[57] O. Grünberg,[66] E. Gushchin,[34] Yu. Guz,[37] T. Gys,[40] C. Göbel,[62] T. Hadavizadeh,[57] C. Hadjivasiliou,[5] G. Haefeli,[41] C. Haen,[40] S. C. Haines,[49] S. Hall,[55] B. Hamilton,[60] X. Han,[12] S. Hansmann-Menzemer,[12] N. Harnew,[57] S. T. Harnew,[48] J. Harrison,[56] M. Hatch,[40] J. He,[63] T. Head,[41] A. Heister,[9] K. Hennessy,[54] P. Henrard,[5] L. Henry,[8] J. A. Hernando Morata,[39] E. van Herwijnen,[40] M. Heß,[66] A. Hicheur,[2] D. Hill,[57] C. Hombach,[56] H. Hopchev,[41] W. Hulsbergen,[43] T. Humair,[55] M. Hushchyn,[35] N. Hussain,[57] D. Hutchcroft,[54] M. Idzik,[28] P. Ilten,[58] R. Jacobsson,[40] A. Jaeger,[12] J. Jalocha,[57] E. Jans,[43] A. Jawahery,[60] F. Jiang,[3] M. John,[57] D. Johnson,[40] C. R. Jones,[49] C. Joram,[40] B. Jost,[40] N. Jurik,[61] S. Kandybei,[45] W. Kanso,[6] M. Karacson,[40] J. M. Kariuki,[48] S. Karodia,[53] M. Kecke,[12] M. Kelsey,[61] I. R. Kenyon,[47] M. Kenzie,[49] T. Ketel,[44] E. Khairullin,[35] B. Khanji,[21,40,i] C. Khurewathanakul,[41] T. Kirn,[9] S. Klaver,[56] K. Klimaszewski,[29] S. Koliiev,[46] M. Kolpin,[12] I. Komarov,[41] R. F. Koopman,[44] P. Koppenburg,[43] A. Kosmyntseva,[32] A. Kozachuk,[33] M. Kozeiha,[5] L. Kravchuk,[34] K. Kreplin,[12] M. Kreps,[50] P. Krokovny,[36,w] F. Kruse,[10] W. Krzemien,[29] W. Kucewicz,[27,l] M. Kucharczyk,[27] V. Kudryavtsev,[36,w] A. K. Kuonen,[41] K. Kurek,[29] T. Kvaratskheliya,[32,40] D. Lacarrere,[40] G. Lafferty,[56] A. Lai,[16] D. Lambert,[52] G. Lanfranchi,[19] C. Langenbruch,[9] T. Latham,[50] C. Lazzeroni,[47] R. Le Gac,[6] J. van Leerdam,[43] J.-P. Lees,[4] A. Leflat,[33,40] J. Lefrançois,[7] R. Lefèvre,[5] F. Lemaitre,[40] E. Lemos Cid,[39] O. Leroy,[6] T. Lesiak,[27] B. Leverington,[12] Y. Li,[7] T. Likhomanenko,[35,67] R. Lindner,[40] C. Linn,[40] F. Lionetto,[42] B. Liu,[16] X. Liu,[3] D. Loh,[50] I. Longstaff,[53] J. H. Lopes,[2] D. Lucchesi,[23,o] M. Lucio Martinez,[39] H. Luo,[52] A. Lupato,[23] E. Luppi,[17,g] O. Lupton,[57] A. Lusiani,[24] X. Lyu,[63] F. Machefert,[7] F. Maciuc,[30] O. Maev,[31] K. Maguire,[56] S. Malde,[57] A. Malinin,[67] T. Maltsev,[36] G. Manca,[7] G. Mancinelli,[6] P. Manning,[61] J. Maratas,[5,v] J. F. Marchand,[4] U. Marconi,[15] C. Marin Benito,[38] P. Marino,[24,t] J. Marks,[12] G. Martellotti,[26] M. Martin,[6] M. Martinelli,[41] D. Martinez Santos,[39] F. Martinez Vidal,[68] D. Martins Tostes,[2] L. M. Massacrier,[7] A. Massafferri,[1] R. Matev,[40] A. Mathad,[50] Z. Mathe,[40] C. Matteuzzi,[21] A. Mauri,[42] B. Maurin,[41] A. Mazurov,[47] M. McCann,[55] J. McCarthy,[47] A. McNab,[56] R. McNulty,[13] B. Meadows,[59] F. Meier,[10] M. Meissner,[12] D. Melnychuk,[29] M. Merk,[43] A. Merli,[22,q] E. Michielin,[23] D. A. Milanes,[65] M.-N. Minard,[4] D. S. Mitzel,[12] A. Mogini,[8] J. Molina Rodriguez,[62] I. A. Monroy,[65] S. Monteil,[5] M. Morandin,[23] P. Morawski,[28] A. Mordà,[6] M. J. Morello,[24,t] J. Moron,[28] A. B. Morris,[52] R. Mountain,[61] F. Muheim,[52] M. Mulder,[43] M. Mussini,[15] D. Müller,[56] J. Müller,[10] K. Müller,[42] V. Müller,[10] P. Naik,[48] T. Nakada,[41] R. Nandakumar,[51] A. Nandi,[57] I. Nasteva,[2] M. Needham,[52] N. Neri,[22] S. Neubert,[12] N. Neufeld,[40] M. Neuner,[12] A. D. Nguyen,[41] C. Nguyen-Mau,[41,n] S. Nieswand,[9] R. Niet,[10] N. Nikitin,[33] T. Nikodem,[12] A. Novoselov,[37] D. P. O'Hanlon,[50] A. Oblakowska-Mucha,[28] V. Obraztsov,[37] S. Ogilvy,[19]

R. Oldeman,[49] C. J. G. Onderwater,[69] J. M. Otalora Goicochea,[2] A. Otto,[40] P. Owen,[42] A. Oyanguren,[68] P. R. Pais,[41] A. Palano,[14,d] F. Palombo,[22,q] M. Palutan,[19] J. Panman,[40] A. Papanestis,[51] M. Pappagallo,[14,d] L. L. Pappalardo,[17,g] W. Parker,[60] C. Parkes,[56] G. Passaleva,[18] A. Pastore,[14,d] G. D. Patel,[54] M. Patel,[55] C. Patrignani,[15,e] A. Pearce,[56,51] A. Pellegrino,[43] G. Penso,[26] M. Pepe Altarelli,[40] S. Perazzini,[40] P. Perret,[5] L. Pescatore,[47] K. Petridis,[48] A. Petrolini,[20,h] A. Petrov,[67] M. Petruzzo,[22,q] E. Picatoste Olloqui,[38] B. Pietrzyk,[4] M. Pikies,[27] D. Pinci,[26] A. Pistone,[20] A. Piucci,[12] S. Playfer,[52] M. Plo Casasus,[39] T. Poikela,[40] F. Polci,[8] A. Poluektov,[50,36] I. Polyakov,[61] E. Polycarpo,[2] G. J. Pomery,[48] A. Popov,[37] D. Popov,[11,40] B. Popovici,[30] S. Poslavskii,[37] C. Potterat,[2] E. Price,[48] J. D. Price,[54] J. Prisciandaro,[39] A. Pritchard,[54] C. Prouve,[48] V. Pugatch,[46] A. Puig Navarro,[41] G. Punzi,[24,p] W. Qian,[57] R. Quagliani,[7,48] B. Rachwal,[27] J. H. Rademacker,[48] M. Rama,[24] M. Ramos Pernas,[39] M. S. Rangel,[2] I. Raniuk,[45] G. Raven,[44] F. Redi,[55] S. Reichert,[10] A. C. dos Reis,[1] C. Remon Alepuz,[68] V. Renaudin,[7] S. Ricciardi,[51] S. Richards,[48] M. Rihl,[40] K. Rinnert,[54] V. Rives Molina,[38] P. Robbe,[7,40] A. B. Rodrigues,[1] E. Rodrigues,[59] J. A. Rodriguez Lopez,[65] P. Rodriguez Perez,[56,†] A. Rogozhnikov,[35] S. Roiser,[40] A. Rollings,[57] V. Romanovskiy,[37] A. Romero Vidal,[39] J. W. Ronayne,[13] M. Rotondo,[19] M. S. Rudolph,[61] T. Ruf,[40] P. Ruiz Valls,[68] J. J. Saborido Silva,[39] E. Sadykhov,[32] N. Sagidova,[31] B. Saitta,[16,f] V. Salustino Guimaraes,[2] C. Sanchez Mayordomo,[68] B. Sanmartin Sedes,[39] R. Santacesaria,[26] C. Santamarina Rios,[39] M. Santimaria,[19] E. Santovetti,[25,j] A. Sarti,[19,k] C. Satriano,[26,s] A. Satta,[25] D. M. Saunders,[48] D. Savrina,[32,33] S. Schael,[9] M. Schellenberg,[10] M. Schiller,[40] H. Schindler,[40] M. Schlupp,[10] M. Schmelling,[11] T. Schmelzer,[10] B. Schmidt,[40] O. Schneider,[41] A. Schopper,[40] K. Schubert,[10] M. Schubiger,[41] M.-H. Schune,[7] R. Schwemmer,[40] B. Sciascia,[19] A. Sciubba,[26,k] A. Semennikov,[32] A. Sergi,[47] N. Serra,[42] J. Serrano,[6] L. Sestini,[23] P. Seyfert,[21] M. Shapkin,[37] I. Shapoval,[45] Y. Shcheglov,[31] T. Shears,[54] L. Shekhtman,[36,w] V. Shevchenko,[67] A. Shires,[10] B. G. Siddi,[17,40] R. Silva Coutinho,[42] L. Silva de Oliveira,[2] G. Simi,[23,o] S. Simone,[14,d] M. Sirendi,[49] N. Skidmore,[48] T. Skwarnicki,[61] E. Smith,[55] I. T. Smith,[52] J. Smith,[49] M. Smith,[55] H. Snoek,[43] M. D. Sokoloff,[59] F. J. P. Soler,[53] B. Souza De Paula,[2] B. Spaan,[10] P. Spradlin,[53] S. Sridharan,[40] F. Stagni,[40] M. Stahl,[12] S. Stahl,[40] P. Stefko,[41] S. Stefkova,[55] O. Steinkamp,[42] S. Stemmle,[12] O. Stenyakin,[37] S. Stevenson,[57] S. Stoica,[30] S. Stone,[61] B. Storaci,[42] S. Stracka,[24,p] M. Straticiuc,[30] U. Straumann,[42] L. Sun,[59] W. Sutcliffe,[55] K. Swientek,[28] V. Syropoulos,[44] M. Szczekowski,[29] T. Szumlak,[28] S. T'Jampens,[4] A. Tayduganov,[6] T. Tekampe,[10] M. Teklishyn,[7] G. Tellarini,[17,g] F. Teubert,[40] E. Thomas,[40] J. van Tilburg,[43] M. J. Tilley,[55] V. Tisserand,[4] M. Tobin,[41] S. Tolk,[49] L. Tomassetti,[17,g] D. Tonelli,[40] S. Topp-Joergensen,[57] F. Toriello,[61] E. Tournefier,[4] S. Tourneur,[41] K. Trabelsi,[41] M. Traill,[53] M. T. Tran,[41] M. Tresch,[42] A. Trisovic,[40] A. Tsaregorodtsev,[6] P. Tsopelas,[43] A. Tully,[49] N. Tuning,[43] A. Ukleja,[29] A. Ustyuzhanin,[35] U. Uwer,[12] C. Vacca,[16,f] V. Vagnoni,[15,40] A. Valassi,[40] S. Valat,[40] G. Valenti,[15] A. Vallier,[7] R. Vazquez Gomez,[19] P. Vazquez Regueiro,[39] S. Vecchi,[17] M. van Veghel,[43] J. J. Velthuis,[48] M. Veltri,[18,r] G. Veneziano,[41] A. Venkateswaran,[61] M. Vernet,[5] M. Vesterinen,[12] B. Viaud,[7] D. Vieira,[1] M. Vieites Diaz,[39] X. Vilasis-Cardona,[38,m] V. Volkov,[33] A. Vollhardt,[42] B. Voneki,[40] A. Vorobyev,[31] V. Vorobyev,[36,w] C. Voß,[66] J. A. de Vries,[43] C. Vázquez Sierra,[39] R. Waldi,[66] C. Wallace,[50] R. Wallace,[13] J. Walsh,[24] J. Wang,[61] D. R. Ward,[49] H. M. Wark,[54] N. K. Watson,[47] D. Websdale,[55] A. Weiden,[42] M. Whitehead,[40] J. Wicht,[50] G. Wilkinson,[57,40] M. Wilkinson,[61] M. Williams,[40] M. P. Williams,[47] M. Williams,[58] T. Williams,[47] F. F. Wilson,[51] J. Wimberley,[60] J. Wishahi,[10] W. Wislicki,[29] M. Witek,[27] G. Wormser,[7] S. A. Wotton,[49] K. Wraight,[53] S. Wright,[49] K. Wyllie,[40] Y. Xie,[64] Z. Xing,[61] Z. Xu,[41] Z. Yang,[3] H. Yin,[64] J. Yu,[64] X. Yuan,[36,w] O. Yushchenko,[37] K. A. Zarebski,[47] M. Zavertyaev,[11,c] L. Zhang,[3] Y. Zhang,[7] Y. Zhang,[63] A. Zhelezov,[12] Y. Zheng,[63] A. Zhokhov,[32] X. Zhu,[3] V. Zhukov,[9] and S. Zucchelli[15]

(LHCb Collaboration)

[1]*Centro Brasileiro de Pesquisas Físicas (CBPF), Rio de Janeiro, Brazil*
[2]*Universidade Federal do Rio de Janeiro (UFRJ), Rio de Janeiro, Brazil*
[3]*Center for High Energy Physics, Tsinghua University, Beijing, China*
[4]*LAPP, Université Savoie Mont-Blanc, CNRS/IN2P3, Annecy-Le-Vieux, France*
[5]*Clermont Université, Université Blaise Pascal, CNRS/IN2P3, LPC, Clermont-Ferrand, France*
[6]*CPPM, Aix-Marseille Université, CNRS/IN2P3, Marseille, France*
[7]*LAL, Université Paris-Sud, CNRS/IN2P3, Orsay, France*
[8]*LPNHE, Université Pierre et Marie Curie, Université Paris Diderot, CNRS/IN2P3, Paris, France*
[9]*I. Physikalisches Institut, RWTH Aachen University, Aachen, Germany*
[10]*Fakultät Physik, Technische Universität Dortmund, Dortmund, Germany*

[11]*Max-Planck-Institut für Kernphysik (MPIK), Heidelberg, Germany*
[12]*Physikalisches Institut, Ruprecht-Karls-Universität Heidelberg, Heidelberg, Germany*
[13]*School of Physics, University College Dublin, Dublin, Ireland*
[14]*Sezione INFN di Bari, Bari, Italy*
[15]*Sezione INFN di Bologna, Bologna, Italy*
[16]*Sezione INFN di Cagliari, Cagliari, Italy*
[17]*Sezione INFN di Ferrara, Ferrara, Italy*
[18]*Sezione INFN di Firenze, Firenze, Italy*
[19]*Laboratori Nazionali dell'INFN di Frascati, Frascati, Italy*
[20]*Sezione INFN di Genova, Genova, Italy*
[21]*Sezione INFN di Milano Bicocca, Milano, Italy*
[22]*Sezione INFN di Milano, Milano, Italy*
[23]*Sezione INFN di Padova, Padova, Italy*
[24]*Sezione INFN di Pisa, Pisa, Italy*
[25]*Sezione INFN di Roma Tor Vergata, Roma, Italy*
[26]*Sezione INFN di Roma La Sapienza, Roma, Italy*
[27]*Henryk Niewodniczanski Institute of Nuclear Physics Polish Academy of Sciences, Kraków, Poland*
[28]*AGH - University of Science and Technology, Faculty of Physics and Applied Computer Science, Kraków, Poland*
[29]*National Center for Nuclear Research (NCBJ), Warsaw, Poland*
[30]*Horia Hulubei National Institute of Physics and Nuclear Engineering, Bucharest-Magurele, Romania*
[31]*Petersburg Nuclear Physics Institute (PNPI), Gatchina, Russia*
[32]*Institute of Theoretical and Experimental Physics (ITEP), Moscow, Russia*
[33]*Institute of Nuclear Physics, Moscow State University (SINP MSU), Moscow, Russia*
[34]*Institute for Nuclear Research of the Russian Academy of Sciences (INR RAN), Moscow, Russia*
[35]*Yandex School of Data Analysis, Moscow, Russia*
[36]*Budker Institute of Nuclear Physics (SB RAS), Novosibirsk, Russia*
[37]*Institute for High Energy Physics (IHEP), Protvino, Russia*
[38]*ICCUB, Universitat de Barcelona, Barcelona, Spain*
[39]*Universidad de Santiago de Compostela, Santiago de Compostela, Spain*
[40]*European Organization for Nuclear Research (CERN), Geneva, Switzerland*
[41]*Institute of Physics, Ecole Polytechnique Fédérale de Lausanne (EPFL), Lausanne, Switzerland*
[42]*Physik-Institut, Universität Zürich, Zürich, Switzerland*
[43]*Nikhef National Institute for Subatomic Physics, Amsterdam, The Netherlands*
[44]*Nikhef National Institute for Subatomic Physics and VU University Amsterdam, Amsterdam, The Netherlands*
[45]*NSC Kharkiv Institute of Physics and Technology (NSC KIPT), Kharkiv, Ukraine*
[46]*Institute for Nuclear Research of the National Academy of Sciences (KINR), Kyiv, Ukraine*
[47]*University of Birmingham, Birmingham, United Kingdom*
[48]*H.H. Wills Physics Laboratory, University of Bristol, Bristol, United Kingdom*
[49]*Cavendish Laboratory, University of Cambridge, Cambridge, United Kingdom*
[50]*Department of Physics, University of Warwick, Coventry, United Kingdom*
[51]*STFC Rutherford Appleton Laboratory, Didcot, United Kingdom*
[52]*School of Physics and Astronomy, University of Edinburgh, Edinburgh, United Kingdom*
[53]*School of Physics and Astronomy, University of Glasgow, Glasgow, United Kingdom*
[54]*Oliver Lodge Laboratory, University of Liverpool, Liverpool, United Kingdom*
[55]*Imperial College London, London, United Kingdom*
[56]*School of Physics and Astronomy, University of Manchester, Manchester, United Kingdom*
[57]*Department of Physics, University of Oxford, Oxford, United Kingdom*
[58]*Massachusetts Institute of Technology, Cambridge, Massachusetts, United States*
[59]*University of Cincinnati, Cincinnati, Ohio, USA*
[60]*University of Maryland, College Park, Maryland, USA*
[61]*Syracuse University, Syracuse, New York, USA*
[62]*Pontifícia Universidade Católica do Rio de Janeiro (PUC-Rio), Rio de Janeiro, Brazil,*
associated to Universidade Federal do Rio de Janeiro (UFRJ), Rio de Janeiro, Brazil
[63]*University of Chinese Academy of Sciences, Beijing, China,*
associated to Center for High Energy Physics, Tsinghua University, Beijing, China
[64]*Institute of Particle Physics, Central China Normal University, Wuhan, Hubei, China,*
associated to Center for High Energy Physics, Tsinghua University, Beijing, China
[65]*Departamento de Fisica, Universidad Nacional de Colombia, Bogota, Colombia,*
associated to LPNHE, Université Pierre et Marie Curie, Université Paris Diderot, CNRS/IN2P3, Paris, France

[66]*Institut für Physik, Universität Rostock, Rostock, Germany,
associated to Physikalisches Institut, Ruprecht-Karls-Universität Heidelberg, Heidelberg, Germany*
[67]*National Research Centre Kurchatov Institute, Moscow, Russia,
associated to Institute of Theoretical and Experimental Physics (ITEP), Moscow, Russia*
[68]*Instituto de Fisica Corpuscular (IFIC), Universitat de Valencia-CSIC, Valencia, Spain,
associated to ICCUB, Universitat de Barcelona, Barcelona, Spain*
[69]*Van Swinderen Institute, University of Groningen, Groningen, The Netherlands,
associated to Nikhef National Institute for Subatomic Physics, Amsterdam, The Netherlands*

[†]Deceased.
[a]Universidade Federal do Triângulo Mineiro (UFTM), Uberaba-MG, Brazil.
[b]Laboratoire Leprince-Ringuet, Palaiseau, France.
[c]P.N. Lebedev Physical Institute, Russian Academy of Science (LPI RAS), Moscow, Russia.
[d]Università di Bari, Bari, Italy.
[e]Università di Bologna, Bologna, Italy.
[f]Università di Cagliari, Cagliari, Italy.
[g]Università di Ferrara, Ferrara, Italy.
[h]Università di Genova, Genova, Italy.
[I]Università di Milano Bicocca, Milano, Italy.
[j]Università di Roma Tor Vergata, Roma, Italy.
[k]Università di Roma La Sapienza, Roma, Italy.
[l]AGH - University of Science and Technology, Faculty of Computer Science, Electronics and Telecommunications, Kraków, Poland.
[m]LIFAELS, La Salle, Universitat Ramon Llull, Barcelona, Spain.
[n]Hanoi University of Science, Hanoi, Vietnam.
[o]Università di Padova, Padova, Italy.
[p]Università di Pisa, Pisa, Italy.
[q]Università degli Studi di Milano, Milano, Italy.
[r]Università di Urbino, Urbino, Italy.
[s]Università della Basilicata, Potenza, Italy.
[t]Scuola Normale Superiore, Pisa, Italy.
[u]Università di Modena e Reggio Emilia, Modena, Italy.
[v]Iligan Institute of Technology (IIT), Iligan, Philippines.
[w]Novosibirsk State University, Novosibirsk, Russia.